Plankton Reach New Heights in Effort to Avoid Predators

Brad J. Gemmell[1], Houshuo Jiang[2], J. Rudi Strickler[3], Edward J. Buskey[1]

[1]University of Texas at Austin Marine Science Institute, [2]Woods Hole Oceanographic Institution, [3]University of Wisconsin Milwaukee.

ABSTRACT

The marine environment associated with the air-water interface (neuston) provides an important food source to pelagic organisms where subsurface prey is limited. However, studies on predator-prey interactions within this environment are lacking. Copepods are known to produce strong escape jumps in response to predators but must contend with a low Reynolds number environment where viscous forces limit escape distance. All previous work on copepods interaction with predators has focused on a liquid environment. Here, we describe a novel anti-predator behavior in two neustonic copepod species where individuals frequently exit the water surface and travel many times their own body length through air to avoid predators. Using both field recordings with natural predators and high speed laboratory recordings we obtain detailed kinematics of this behavior, and estimate energetic cost associated with this behavior. We demonstrate that despite losing up to 88% of their initial kinetic energy, copepods which break the water surface travel significantly further than escapes underwater and successfully exit the perceptive field of the predator. This behavior provides an effective defense mechanism against subsurface feeding visual predators and the results provide insight into trophic interactions within the neustonic environment.

1. INTRODUCION

Copepods are one of the most abundant metazoans on the planet [1-2] and are known to be important prey for fish [3-6] and other marine organisms [7-8]. The copepod's role in marine food webs makes their behavioral adaptations to predation important to understand. The neustonic environment consists of the upper few millimeters of water associated with the air-water interface. This environment is often characterized by elevated biomass and numbers of organisms relative to the water beneath [9] and provides food to higher tropic levels such as fish [10]. Pontellid copepods are a ubiquitous group often found in neustonic environments and

adults are known to reside during daylight hours in the brightly lit surface water of coastal oceans [11].

Many planktonic organisms residing in the photic zone have nearly transparent tissues which are assumed to reduce conspicuousness to visual predators [12]. However, species which live in close proximity to the water surface (neuston) are often highly pigmented, including copepods [13]. Pigmentation in copepods has been demonstrated to reduce the effects of damaging UV radiation [14-15] and may play a similar role in Pontellids. These copepods are also large in comparison with many other copepod taxa [16]. This large size combined with pigmentation makes these copepods more visually conspicuous and thus, should be preferred by visual fish predators [17-18].

One of the mechanisms by which copepods are known to avoid fish predators is through the use of powerful escape jumps [19-22]. These escape jumps are present throughout development [23-24] and can generate speeds up to 800 mm s^{-1} and accelerations of up to 200 m s^{-2} [20]. The interaction of copepods and their natural predators has been investigated in a liquid medium [22, 25-26]. However aerial escapes have never been investigated for a planktonic organism but may have significant ecological and evolutionary implications for the wide variety of species that live and feed within the surface layer of the ocean.

Reports of copepods breaking through the water surface occurred as early as the late 19^{th} century [27]. The observer hypothesized that the leaps into the air and subsequent re-entry into the water functioned as a mechanism to assist with molting, by jarring them loose from their old exoskeleton. A later report of aerial copepod jumps proposed an anti-predator mechanism [28], but the function of this behavior remained hypothetical.

55 Using field video recordings and high speed video in the laboratory, we demonstrate that
56 aerial jumps provide an effective escape mechanism in response to visual fish predators.
57 Kinematic analysis of this little known behavior reveals a significant energetic cost of breaking
58 the water surface, yet this aerial escape behavior still provides a net energy savings relative to an
59 escape performed solely underwater. These findings provide insight into how this group of
60 animals can be successful in a pelagic environment where they appear conspicuous and easily
61 targeted by visual predators.

62 **2. MATERIALS AND METHODS**

63 ***a) Field recordings***

64 Field recordings were made using a hand-held video recorder at 30 frames s^{-1} (Sony
65 Handycam CCD-TR3300) above the water surface. Recordings were edited in Adobe Premier
66 Pro to maximize distinction between copepods and the surrounding water by adjusting both
67 brightness and contrast. Two-dimensional escape kinematics in response to fish predators were
68 obtained using ImageJ v1.43 software. Statistical analysis for both laboratory and field
69 recordings were performed using Sigmaplot 11.0 (Systat Software Inc).

70 Field recordings of the copepod, *Anomalocera ornata* interacting with juvenile mullet
71 (*Mugil cephalus*) were performed for 15 min at the University of Texas Marine Science Institute
72 marina and escape responses from 89 individuals were obtained during analysis. The movement
73 of the camera required to follow individual fish interacting with copepods made simple size and
74 distance calibrations inappropriate. Instead, we captured and measured 22 of the juvenile *M.*
75 *cephalus* that were in the location of the video recordings and the resulting standard length of
76 24.2 mm (SD 1.96) was used to scale the video frames during kinematic analysis. This method
77 does not provide the finest spatial resolution but allows a reasonable approximation of both

distance and velocity. It should be noted that the calculated kinematic values represent minimum estimates of both velocity and distance since recordings were based solely in an X-Y plane normal to the camera lens so any Z component of motion was not accounted for. Therefore, velocity and distance are likely underestimated but this effect is minimal for the laboratory studies since the narrow (4 cm width) aquarium limited movement in the Z plane.

b) Laboratory recordings

Copepods (*Labidocera aestiva*) were collected from inshore waters of the Northern Gulf of Mexico (27° 50' 19" N 97° 3' 8" W) using a 0.5 m diameter plankton net (150 µm mesh). Approximately 50 individuals were placed in a small, narrow rectangular acrylic aquarium (20cm x 4cm x 20cm) filled to 50% capacity with filtered seawater. A high speed camera, Redlake MotionMeter® model 1140-0003 equipped with a Nikon Nikkor 55-mm lens was used to capture the escape behavior. Dark field illumination was provided by infrared light emitting diodes (peak wavelength 890 nm). The copepod escape jumps were recorded at 250-500 frames s^{-1}. After 10 recordings, copepods were replaced with 50 new animals to limit the probability of recording the same animal multiple times.

Two camera positions were utilized during laboratory recordings. In position 1 the camera was aligned with the aquarium so that the surface of the water was near the bottom of the field of view in order to capture the entire aerial portion of the escape and 60 escapes were recorded using this configuration. In position 2 the camera was oriented so that approximately $1/3^{rd}$ of the field of view was below the surface of the water and $2/3^{rds}$ were above the water surface. This allowed determination of the copepod's speed as it broke the water's surface, the contact angle to the surface and the trajectory through air. 24 escapes were recorded with this configuration. The contact angle was determined at the instant contact was made at the water

surface, while the entire animal remained underwater. Using image analysis software (ImageJ) we determined the angle using the water surface and the longitudinal central plane of the animal. Recordings were performed in a darkroom and escape responses from the copepods were elicited through a photic startle response by a rapid change in light intensity [29]. The subsequent escape responses resulted in many copepods breaking the water's surface and traveling variable distances through the air. Escapes in which more than 50% of the aerial trajectory was out of the field of view were not used for analysis. In cases where only a smaller portion (less than 50%) of the escape traveled beyond the field of view, the maximal distance was extrapolated using Vogel's model for an object in free fall [30]. This was required for 19 of the 60 escapes used in our analysis.

c) Data analysis

To compare the kinematic results obtained from both ImageJ v1.43 software and Celltrak v1.5 motion analysis software, data was log transformed and checked for normality using a Shapiro-Wilk test. A one-way analysis of variance (ANOVA) was performed for both total horizontal distance and maximum velocity.

We used the following equation to estimate the net kinetic energy loss (ΔK) incurred from a copepod breaking the water surface:

$$\Delta K = 0.5\, m_{\text{copepod}} \left(U_0^{\,2} - U_1^{\,2} \right) \qquad (1)$$

where m_{copepod} is the body mass of the copepod, U_0 is the copepod velocity at the moment just before the copepod starts to break the water surface, and U_1 is the copepod velocity at the moment right after the copepod becomes completely airborne. $m_{\text{copepod}} = \rho_{\text{copepod}} \times V_{\text{copepod}}$, where ρ_{copepod} is the mass density of the copepod (approximately equal to the mass density of the

seawater, $\rho_{seawater}$), and $V_{copepod}$ is the copepod body volume. $V_{copepod}$ is calculated as $4/3\pi\eta^2 a^3$, where a is half the prosome length, η the copepod aspect ratio, and assuming the shape of a prolate spheroid with the long axis equal to the prosome length, $2a$, and the short axis equal to $\eta \times 2a$.

Here, we estimate three likely contributions to this energy loss:

(1) The loss due to the water drag can be estimated as:

$$\Delta K_1 = 0.25\, C_d\, \rho_{seawater}\, U_0^{\,2}\, S_e\, d_e \qquad (2)$$

where C_d is the drag coefficient of the equivalent sphere having the same volume as that of the copepod body, S_e is the cross-sectional area of the equivalent sphere, and d_e is the diameter of the equivalent sphere. We estimate this energy loss during breaking the water surface (very short time scale) as the average between the moment the animal makes contact with the surface (fully underwater), and moment the animal fully breaks free of the surface (fully in air). Here, we assume that the drag acting on the copepod when it just starts to break the water surface is $0.5\, C_d\, \rho_{seawater}\, U_0^2\, S_e$, and the drag acting on the copepod when it just leaves the water surface to become completely airborne is $0.5\, C_d\, \rho_{air}\, U_1^2\, S_e$, where ρ_{air} is the mass density of air. Because $\rho_{air} << \rho_{seawater}$, the average drag for this short time interval is approximately $0.25\, C_d\, \rho_{seawater}\, U_0^2\, S_e$. The average drag multiplied by the distance traveled, d_e, leads to Equation (2). C_d is calculated based on the Reynolds number $Re = U_0\, d_e / \nu_{seawater}$, where $\nu_{seawater}$ is the kinematic viscosity of the seawater. Although we are not sure about the applicability of the commonly used drag law, Equation (2) should give upper bound estimation of the energy loss due to the water drag.

(2) The loss due to the increase of the gravitational potential energy of the copepod body estimated as:

$$\Delta K_2 = m_{\text{copepod}}\, g\, d_{\text{e}} \cos(\alpha) \quad (3)$$

where g is acceleration due to gravity, and α is the exit angle (figure S1).

(3) The loss due to overcoming the surface tension:

$$\Delta K_3 = \sigma\, A_{\text{copepod}} \cos(\theta) \quad (4)$$

where σ (= 0.075 N m^{-1}) is the surface tension for the seawater-air interface, A_{copepod} is the surface area of the copepod, and θ is the contact angle between the copepod body and the seawater surface. Here, we assume that the energy loss is due to the copepod surface condition changing from interfacing with seawater to interfacing with air, i.e. $\Delta K_3 = \left(\sigma_{\text{copepod}-\text{air}} - \sigma_{\text{copepod}-\text{seawater}}\right) A_{\text{copepod}}$, where $\sigma_{\text{copepod-air}}$ and $\sigma_{\text{copepod-seawater}}$ are the surface energies associated with the copepod-air and copepod-seawater interfaces, respectively. Using Young's law for the contact angle, i.e. $\sigma_{\text{copepod-air}} = \sigma_{\text{copepod-seawater}} + \sigma\cos(\theta)$ [31], we obtain Equation (4).

3. RESULTS

Field video recordings captured the copepod *Anomalocera ornata* (prosome length 2.5-3.1 mm) in the presence of small plankton feeding fish (juvenile *Mugil cephalus*) within inshore waters of the Northwestern Gulf of Mexico. The escape behavior was stimulated by the approach of the predatory fish, *M. cephalus,* (figure 1) and consisted of an airborne leap covering a horizontal distance of 80 ±30 mm (N= 89), with maximum distances of up to 170 mm observed (see data supplement for video of this behavior). On average, the copepods travelled over 40 times their own body length and 3.4 times the body length of the fish predator (mean standard length 24.2mm). The maximum aerial velocity achieved during these escapes was 890 ±200 mm

166 s^{-1} and average velocities over the entire escape were 660 ±150 mm s^{-1} (figure 2*a*). Only 1 of the
167 89 observed escapes resulted in multiple attacks by the same fish.

168 A smaller Pontellid copepod (prosome length 1.8-2.0 mm), *Labidocera aestiva*, was
169 stimulated to perform escape jumps in the laboratory using a photic startle response and the
170 escapes were recorded with a high speed video camera at 250-500 frames s^{-1}(see data supplement
171 for video of this behavior). This species swam approximately 0-40 mm below the water's surface
172 until stimulated to escape. We found that maximum aerial velocity of the copepods after they
173 broke the water's surface to be 630 ±150 mm s^{-1}. This was significantly lower (P = <0.001) than
174 velocities produced by *A. ornata* and also resulted in significantly lower (P = <0.001) horizontal
175 escape distances (figure 2*a*). *Labidocera aestiva* was able to attain heights over 60 mm above the
176 water's surface and up to 76 mm in distance from the exit point in the water. However, the mean
177 horizontal distance travelled during escapes through air was 16.0 ±14.1 mm. It is interesting to
178 note that in most cases rotation was imparted on the animal as it broke the surface (see
179 supplemental video). In some cases the rotation was estimated in excess of 45,000 degrees s^{-1}
180 (7500 rpm). The underwater portion of the escapes for *L. aestiva* yielded maximum velocities of
181 1036 ±121 mm s^{-1} which is significantly greater (P = <0.001) than maximum velocities observed
182 after breaking the surface.

183 The results of a correlation analysis between horizontal escape distance and maximum
184 aerial velocity for *A. ornata* exhibited a moderate relationship (R^2= 0.36) (figure 2*b*). The same
185 analysis performed for *L. aestiva* exhibited virtually no correlation between horizontal escape
186 distance and maximum aerial velocity (R^2= 0.04) (figure 2*c*). Notably, swimming pattern and
187 orientation of the two species relative to the water surface before escape is also different (figure
188 3). *L. aestiva* was observed to swim freely below the water surface using an intermittent

189 (cruising-sinking) swimming pattern. During the cruising phase, the copepod was oriented
190 randomly to the water surface but during sinking, *L. aestiva* was consistently observed to orient
191 with its anterior end towards the water surface. *A. ornata* exhibited a cruising swimming pattern
192 and was consistently oriented with its ventral side facing downwards (away from the surface)
193 and the dorsal side of the animal at the water surface.

194 When high speed recordings during the aerial portion of an escape jump of *L. aestiva* are
195 compared to a model of biological projectiles [29] the copepod acts as a ballistic object in free-
196 fall (figure 4*a*). Using data from both 500 fps and 250 fps observations, we estimate that 58-
197 88% of the kinetic energy at the moment when the copepod starts to break the water surface will
198 be lost for breaking the water surface (figure 4*b*). Among the total loss (fit to the data), 61-67%
199 is due to overcoming the water drag force (i.e. ΔK_1), the contribution from increases of
200 gravitational potential energy (ΔK_2) is negligible, and the loss due to overcoming the surface
201 tension (ΔK_3) is 33-39%. When a similar calculation is made for adult flying fish which are
202 orders of magnitude larger than Pontellid copepods, yet produce a functionally analogous
203 behavior, the cost of breaking the surface is < 0.07% of the kinetic energy possessed at the
204 moment when the fish starts to break the water surface.

205 **4. DISCUSSION**

206 Large scale movement of copepods that reside in the neustonic surface layer of the ocean
207 is often subject to surface currents. They have been observed to accumulate at oceanic frontal
208 boundaries [32] where small predatory fish are also more abundant [33]. Thus, successful
209 predator evasion is essential to the copepod's survival. However being confined at the surface
210 limits escape ability and predators have been observed using the water surface to aid in prey
211 capture [34]. The ability of some Pontellid copepods to break the water surface provides

advantages over escapes which occur solely underwater. First, exiting the perceptive field of a predator and re-entering at a random location reduces the chance of continued pursuit and the 80 ±30 mm horizontal escape distance observed for *A. ornata* is well beyond the perceptive distance determined for fish of the similar length to *C. mugil* [35]. Second, for a copepod to achieve a similar escape distance solely underwater, it would have to expend ~20 times more mechanical energy, therefore a significant energetic savings exists by jumping into air.

The underwater velocity is higher than maximum velocities reported for other similarly sized copepods [20] which facilitate these small organisms breaking the water surface. However, the mode in which the two species of copepods exit the water is different (figure 3). *A. ornata* consistently swims with its dorsal side at the water surface while the anterior end of *L. aestiva* was generally directed toward the surface but was observed to swim at many orientations just below the surface. This may explain why *L. aestiva* exhibits a lower correlation between maximum aerial velocity and horizontal distance than *A. ornata* (figure 2*b*, *c*).

Considering a single stroke escape jump that occurs completely underwater, the copepod achieves its peak velocity approximately at the end of the power stroke of the swimming legs. During the power stroke, the copepod travels a distance n*L*, where *L* is the prosome length and n ~ 1-2 [21]. Upon completion of the power stroke, the copepod rapidly decelerates due to drag forces but maintains enough inertia to move forward another distance of ~n*L* until coming to rest. The present observations show that copepods, via a one-kick jump, can break the surface of the water (see supplemental video) and peak velocity (U_0) is obtained just before breaking the surface. At the moment when the animal becomes completely airborne it travels at a velocity (U_1), which is significantly smaller than U_0. In other words, there is a net kinetic energy loss

(figure 4*b*). The net kinetic energy loss (ΔK) incurred during the copepod *Labidocera aestiva* breaking the water surface is 58-88%.

This energy loss, however, is compensated for by increased escape distance. After becoming airborne, the copepod can travel significantly farther than n*L* (i.e. the distance it otherwise travels underwater) because it now experiences the air mass density, which is ~850 times smaller than the mass density of seawater. Therefore, the copepod will experience less drag resulting in increased distance. There is no propulsive force exerted by the copepod after it becomes airborne, and the copepod undergoes ballistic motion because of gravity (and the air drag force) (figure 4a).

Our field observations show that copepods can effectively use aerial escapes as an anti-predator mechanism. By leaving the perceptive environment of the visual fish predators and re-entering the water up to 170 mm (≈60 body lengths) away from the attack site, a copepod can utilize this effective strategy which appears analogous to that of some larger organisms (e.g. flying fish). An important difference, however, is that all species known to perform similar types of behavior are orders of magnitude larger than copepods. This means that copepods must contend with the reduced inertial forces (lower Reynolds number) and a greater proportion of the total energy dedicated to break the surface tension of water.

Consider the case of a flying fish. We calculate that flying fish lose <0.07% of their overall kinetic energy breaking the surface tension compared to 33-39% in the case of the copepod, despite a greater magnitude of energy loss (due to larger surface area) than copepods. This is due to the fact that flying fish possess orders of magnitude more kinetic energy upon contact with the water surface because of much greater mass and underwater speeds of ≈10 m s^{-1} [36], compared to ≈1 m s^{-1} in copepods. However, it should be noted that although aerial escapes

in larger, heavier aquatic animals lose almost no kinetic energy from surface tension effects, horizontal distances in terms of body length (for animals exhibiting ballistic aerial motion) are much shorter [37]. Thus, what appears to be a disadvantage of small mass (e.g. losing significant proportion of kinetic energy) can translate into an advantage: once the water surface is broken, the copepod travels disproportionally farther than larger animals (with ballistic flight paths). The major reason for this is that the copepod has the ability to generate and maintain a disproportionally large air-entry velocity (relative to body length) compared to larger animals. A secondary reason might be that the flying copepod experiences smaller air drag-induced deceleration than larger animals. Therefore ballistic aerial escape paths can be effective in pelagic ecosystems when the animal (and predator) is small, but are unlikely to carry a larger animal out of the perceptive range of their predator. Instead, specialized structures and behavior such as those observed in flying fish are required to extend horizontal distance above water.

Because escapes are energetically costly [38-40], a copepod's fitness can be reduced even without being captured by a predator. It therefore benefits the copepod to balance predation risk and energy cost by avoiding unnecessary escapes. To avoid pursuit or multiple attacks from a predator, copepods must travel to a distance outside of the perceptive range of the predator. During an escape, a copepod travels approximately 1-2 times its prosome length per stroke (calculated from [21]). For the Pontellid copepods this would result in a distance of 2-6 mm per stroke. However, even small fish can perceive prey at least 10 mm away [35, 41] thus; multiple escape jumps are required for a copepod to exit the predator's perceptive field. Therefore, if an escape occurs in air rather than water, reduced drag forces can extend escape distance. This can transport a copepod further from a predator with a single escape jump, than with multiple jumps

279 in an aqueous environment, resulting in net energy savings. They also return to the water in an
280 unpredictable location making pursuit from the predators unlikely.

281 Finally, the Pontellid copepods may have special adaptations to make it easier for them to
282 jump out of the water: One possible adaptation is that the body surface of those copepod species
283 that do perform such air-entering jumps is less wettable than other copepods or crustaceans in
284 general and thus, their surface properties may be essential for their unusual capability of
285 breaking the water surface. Our kinetic energy budget calculation suggests that if the surface
286 tension is not altered during the breaking of the surface (i.e. a constant $\sigma = 0.075$ N m^{-1}), in order
287 to maintain a useful level of kinetic energy after breaking the surface the copepod body surface
288 has to be hydrophobic, i.e. much larger contact angle in the 68-81° range [Fig. 4b; calculated
289 according to Equation (4)]. Another suspected adaptation may be that the copepods inject
290 chemicals during breaking of the surface to reduce the surface tension by 3-6 times, and
291 therefore a useful level of air-entry kinetic energy can still be maintained even when the contact
292 angle remains similar to published measurements for other crustaceans in the range of below 20°
293 [42]. Further investigation is required to find out if these adaptations indeed exist. Nevertheless,
294 unusual morphological structures are known to exist on the dorsal side of Pontellid copepods
295 [43], which might contribute to making the copepod body surface less wettable. However, these
296 morphological structures make up only a small part of the animal's total surface and
297 alternatively, pores specialized for secretion onto the body surface exist in Pontellids [44].
298 Similar pores with currently unknown function may also be involved in secreting substances
299 presumably to alter surface properties or surface tension of water immediately surrounding the
300 animal. Regardless of the mechanism, escaping through air appears to be an effective strategy to
301 not only avoid and survive attacks from predators by temporarily exiting the liquid environment

and exiting the predator's perceptive field, but also to conserve energy during escapes, providing a competitive advantage for Pontellid copepods in the neustonic environment.

Acknowledgements:

This work was supported by grants from the National Science Foundation, USA to EJB (NSF OCE-0452159), to HJ (NSF OCE-1129496). C. Brown assisted BJG with collection and E. Hing-Fay maintained copepods for JRS.

Figure legends:

Figure 1. Representative diagram showing the copepod, *Anomalocera ornata*, response to the approach of a planktivorous fish predator (juvenile *Mugil cephalus*). The fish swims in a random cruising pattern just below the water surface until visually encountering a copepod. a) Once located visually, the fish swims toward the copepod and attempts to ingest it. b) The approach of the fish alerts the copepod to the presence of a potential predator and the copepod responds with an aerial leap. c) The copepod travels many times its own body length and significantly further than a single escape underwater to exit the perceptive field of the predator. d) Once the copepod re-enters the water it resumes swimming at the surface. Note: Not drawn to scale.

Figure 2. a) Relationship between horizontal distance and maximum aerial velocity for two species of copepods during airborne escapes. *Anomalocera ornata* exhibits a significantly greater horizontal distance ($P = <0.001$, $\alpha = 0.050$: 1.000 One-way ANOVA) and aerial velocity ($P = <0.001$, $\alpha = 0.050$: 1.000 One-way ANOVA) than *Labidocera aestiva*. The larger copepod, *A. ornata*, is able to travel proportionally further per unit energy. Note: maximum aerial velocity was obtained at the moment the animal fully exited the water surface. Error bars represent Standard Deviation. b) Regression plot for *A. ornata* ($R^2 = 0.36$) and c) *L. aestiva* ($R^2 = 0.04$), where *A. ornata* shows a stronger correlation of velocity with distance.

Figure 3. Two observed techniques utilized by neustonic copepods to break through surface tension of seawater during aerial escape responses. a) *Labidocera aestiva* swims below the surface and is often oriented with the anterior portion of its body toward the water surface (1). b) *Anamolcera ornata* swims at the air-water interface with its dorsal side facing the surface and ventral side facing downwards (1). After being stimulated to perform an escape, swimming appendages (pereiopods) of both species beat sequentially as antennae fold against the body as the animal is propelled forward (2). As the animals accelerate, the increase in kinetic energy allows the body to overcome surface tension forces and travel through the air (3).

Figure 4. a) Observed copepod trajectory during airborne versus a ballistic/free-fall model prediction. b) Kinetic energy loss as a function of the copepod (maximum) speed below water surface. The squares label the data obtained via 500-frames-per-second video recording, and the triangles label the data obtained via 250-frames-per-second video recording. The solid green line is a fit to the data ($\Delta K = 1.26\text{x}10^{-7}\ U_0^2$, where U_0 is the copepod speed below water surface). The solid blue line is the contribution to the kinetic energy loss due to water drag. The solid red line is the difference between the green line and the blue line. The 2 dashed horizontal lines represent, respectively, the work needed to overcome the surface tension in order for the copepod to be airborne for 2 assumed receding contact angles between the copepod and the seawater interface [calculated from Equation (4) for a constant $\sigma = 0.075$ N m^{-1}]. Note that the red line is bounded between these 2 dashed horizontal lines. Copepod prosome length = 1.8 mm, and aspect ratio = 0.32.

References:

1. Humes, A. G. 1994 How many copepods? *Hydrobiologia*, **292/293**, 1–7. (DOI 10.1007/BF00229916)
2. Turner, J. T. 2004. The importance of small planktonic copepods and their roles in pelagic marine food webs. *Zool. Stud.* **43**, 255–266.
3. Govoni, J. J. & Chester, A. J. 1990. Diet composition of larval *Leiostomus xanthurus* in and about the Mississippi River plume. *J. Plankton Res.* **12**, 819-830. (DOI 10.1093/plankt/12.4.819)
4. Anderson, J. T. 1995. Feeding ecology and condition of larval and pelagic juvenile redfish *Sebastes spp*. *Mar. Ecol. Prog. Ser.* **104**, 211-226.
5. Hillgruber, N., Haldorson, L. J. & Paul, A. J. 1995. Feeding selectivity of larval walleye pollock *Theragra chalcogramma* in the oceanic domain of the Bering Sea. *Mar. Ecol. Prog. Ser.* **120**, 1-10. (DOI 10.3354/meps120001)
6. Conway, D., Coombs, S. H. & Smith, C. 1998. Feeding of anchovy *Engraulis encrasicolus* larvae in the northwestern Adriatic Sea in response to changing hydrobiological conditions. *Mar. Ecol. Prog. Ser.* **175,** 35–49. (DOI 10.3354/meps175035)
7. Costello, J. H, & Colin, S. P. 1994. Morphology, fluid motion and predation by the scyphomedusa *Aurelia aurita*. *Mar Biol.* **121**, 327–334. (DOI 10.1007/BF00346741)
8. Oresland, V. 1995. Winter population structure and feeding of the chaetognath *Eukrohnia hamate* and the copepod *Euchaeta antarctica* in Gerlache Strait, Antarctic Peninsula. *Mar. Ecol. Prog. Ser.* **119**, 77-86. (DOI 10.3354/meps119077)
9. Sieburth, J. M., P.-J. Willis, K. M. Johnson, C. M. Burney, D. M. Lavoie, K. R. Hinga, D. A. Carson, F. W. French III, P. W. Johnson, & P. G. Dairs. 1976. Dissolved organic matter and heterotrophic microneuston in the surface microlayers of the North Atlantic. *Science* **194**, 1415-1418. (DOI 10.1126/science.194.4272.1415)
10. Brodeur, R. D. 1989. Neustonic feeding by juvenile salmonids in coastal waters of the Northeast Pacific. *Can. J. Zool.* **67**, 1995–2007. (DOI 10.1139/z89-284)
11. Tester, P. A., Cohen, J. H. & Cervetto, G. 2004. Reverse vertical migration and hydrographic distribution of *Anomalocera ornata* (Copepoda: Pontellidae) in the US south Atlantic bight. *Mar. Ecol. Prog. Ser.* **268**, 195–203. (DOI 10.3354/meps268195)
12. Hansson, L. A. 2000. Induced pigmentation in zooplankton: a trade-off between threats from predation and ultraviolet radiation. *Proc. R. Soc. Lond.* **267**, 2327-2332. (DOI 10.1098/rspb.2000.1287)
13. Herring, P. J. 1965. Blue pigment of a surface-living oceanic copepod. *Nature.* **205**, 103–104. (DOI 10.1038/205103a0)
14. Byron, E. R. 1982. The adaptive significance of Calanoid copepod pigmentation: a comparative & experimental analysis. *Ecology* **63**, 1871–1886. (DOI 10.2307/1940127)
15. Hansson, L. A., Hylander, S. & Sommaruga, R. 2007. Escape from UV threats in zooplankton: A cocktail of behavior and protective pigmentation. *Ecology* **88**, 1932–1939. DOI 10.1890/06-2038.1)
16. Mauchline, J. 1998. *The Biology of Calanoid Copepods. Advances in Marine Biology*. Vol. 33. Academic Press, San Diego.
17. Brooks, J. L. & Dodson, D. I. 1965. Predation, body size, and composition of the plankton. *Science* **150,** 28–35. (DOI 10.1126/science.150.3692.28)

18. Morgan, S. G. & Christy, J. H. 1996. Survival of marine larvae under the countervailing selective pressures of photodamage and predation. *Limnol. Oceanogr.* **41**, 498-504. (DOI 10.4319/lo.1996.41.3.0498)
19. Buskey, E. J., Lenz, P. H. & Hartline, D. K. 2002. Escape behavior of copepods in response to hydrodynamic disturbances: high speed video analysis. *Mar. Ecol. Prog. Ser.* **235**, 135–146. (DOI 10.3354/meps235135)
20. Lenz, P. H., Hower, A. E. & Hartline, D. K. 2004. Force production during pereiopod power strokes in *Calanus finmarchicus. J. Mar. Systems.* **49**, 133-144. (DOI doi:10.1016/j.jmarsys.2003.05.006)
21. Waggett, R. J. & Buskey, E. J. 2007. Calanoid copepod escape behavior in response to a visual predator. *Mar. Biol.* **150**, 599–607. (DOI 10.1007/s00227-006-0384-3)
22. Viitasalo, M., Kiørboe, T., Flinkman, J., Pedersen, L. W. & Visser, A. W. 1998. Predation vulnerability of planktonic copepods: consequences of predator foraging strategies and prey sensory abilities. *Mar. Ecol. Prog. Ser.* **175**, 129–142. (DOI 10.3354/meps175129)
23. Buskey, E. J. 1994. Factors affecting feeding selectivity of visual predators on the copepod *Acartia tonsa:* locomotion, visibility and escape responses. *Hydrobiol.* **292/293**, 447-453. (DOI 10.1007/BF00229971)
24. Titelman, J. & Kiørboe, T. 2003. Predator avoidance by nauplii. *Mar. Ecol. Prog. Ser.* **247,** 137–149. (DOI 10.3354/meps247137)
25. Waggett, R. J. & Buskey, E. J. 2007. Copepod escape behavior in non-turbulent and turbulent hydrodynamic regimes. *Mar. Ecol. Prog. Ser.* **334**, 193-198. (DOI 10.3354/meps334193)
26. Ohman, M. D. 1986. Predator-limited population growth of the copepod *Pseudocalanus* sp. *J. Plankton Res.* **8**, 673–713. (DOI 10.1093/plankt/8.4.673)
27. Astroumoff, A. 1894. A Flying Copepod. *J. R. Microsc. Soc*. London. p618.
28. Zaitsev, Y. P. 1971. Marine neustonology. VA: National Marine Fisheries Service, NOAA and National Science Foundation, National Technical Information Service.
29. Buskey, E. J. & Hartline, D. K. 2003. High speed video analysis of the escape responses of the copepod *Acartia tonsa* to shadows. *Bio. Bull.* **204**, 28–37.
30. Vogel, S. 2005 Living in a physical world II. The bio-ballistics of small projectiles; *J. Biosci*. **30** 167–175. (DOI 10.1007/BF02703696)
31. de Gennes, P. G., Brochard-Wyart, F. & Quéré, D. 2003. Capillarity and Wetting Phenomena: Drops, Bubbles, Pearls, Waves. Springer, New York.
32. Turner, J. T., Tester, P. A. & Hettler, W. F. 1985. Zooplankton feeding ecology. *Mar. Biol.* **90**, 1-8. (DOI 10.1007/BF00428208)
33. Govoni, J. J. & Grimes C. B. 1992. The surface accumulation of larval fishes by hydrodynamic convergence within the Mississippi River plume front. *Cont. Shelf Res.* **12**, 1265–1276. (DOI 10.1016/0278-4343(92)90063-P)
34. Bonfil, R. 2009. The Biology and Ecology of the Silky Shark, *Carcharhinus Falciformis*, in Sharks of the Open Ocean: Biology, Fisheries and Conservation (eds M. D. Camhi, E. K. Pikitch and E. A. Babcock), Blackwell Publishing Ltd., Oxford, UK. (DOI 10.1002/9781444302516.ch10)
35. Miller, T. J., Crowder, L. B. & Rice J. A. 1993. Ontogenetic changes in behavioural and histological measures of visual acuity in three species of fish. *Environ. Biol. Fishes* **37**, 1–8. (DOI 10.1007/BF00000707)

36. Davenport, J. 1994. How and why do flying fish fly? *Rev. Fish Biol. Fisheries* **4**, 184–214.
37. Saidel, W. M., Strain G. F. & Fornari S. K. 2004. Characterization of the Aerial Escape Response of the African Butterfly Fish, *Pantodon buchholzi* Peters. *Environ. Biol. Fishes* **71**, 63-72.
38. Strickler J. R. 1975. Swimming of planktonic *Cyclops* species (Copepoda, Crustacea): Pattern, movements and their control. In Wu.T.Y.T., Brokaw. C. J. & Brennen. C. (eds), *Swimming and Flying in Nature.* Plenum Press, Princeton, p613.
39. Alcaraz, M. & Strickler, J. R. 1988. Locomotion in copepods: patterns of movement and energetic of *Cyclops. Hydrobiol.* **167/168,** 409-414. (DOI 10.1007/BF00026333)
40. Marrase, C., Costello, J. H., Granata, T. & Strickler, J. R. 1990. Grazing in a turbulent environment: Energy dissipation, encounter rates, and efficacy of feeding currents in *Centropages hamatus*. *Proc. Natl. Acad. Sci. USA* **87**, 1653-1657.
41. Hunt von Herbing, I. & Gallager, S. M. 2000. Foraging behavior in early Atlantic cod larvae *(Gadus morhua)* feeding on a protozoan *(Balanion* sp.) and a copepod nauplius *(Pseudodiaptomus* sp.). *Mar. Biol.* **136**, 591–602. (DOI 10.1007/s002270050719)
42. Becker, K., Hormchong, T. & Wahl, M. 2000. Relevance of crustacean carapace wettability for fouling. *Hydrobiologia*. **426**, 193–201. (DOI 10.1023/A:1003918512565)
43. Ianora, A., Miralto, A. & Vanucci, S. 1992. The surface attachment structure: a unique type of integumental formation in neustonic copepods. *Mar. Biol.* **113**, 401-407. (DOI 10.1007/BF00349165)
44. Blades, P. I. & Youngbluth, M. J. 1979. Mating behavior of *Labidocera aestiva* (Copepoda: Calanoida). *Mar. Biol.* **51**, 339-355.

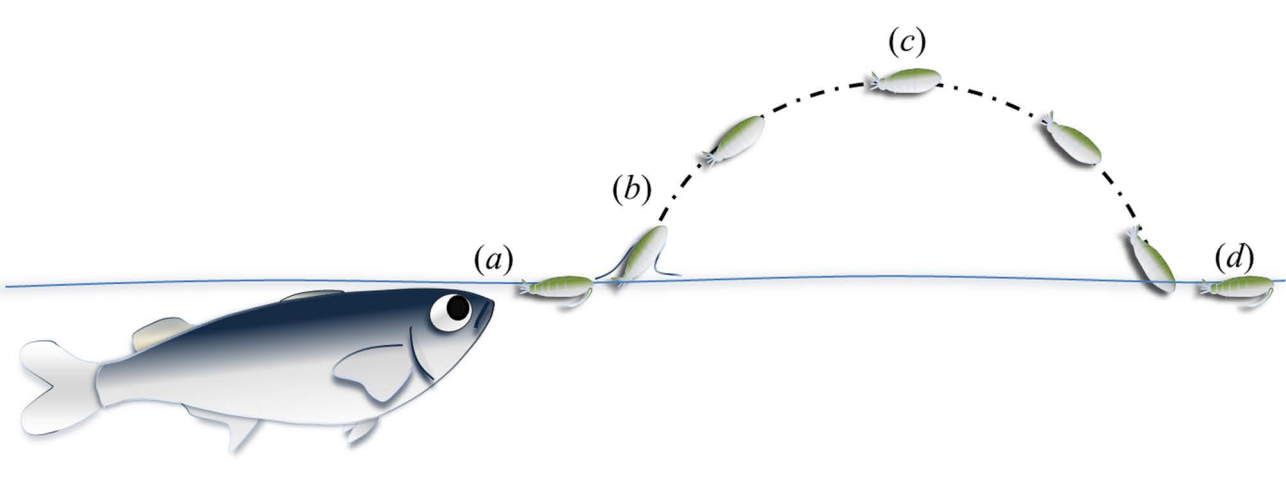
(a)
(b)
(c)
(d)

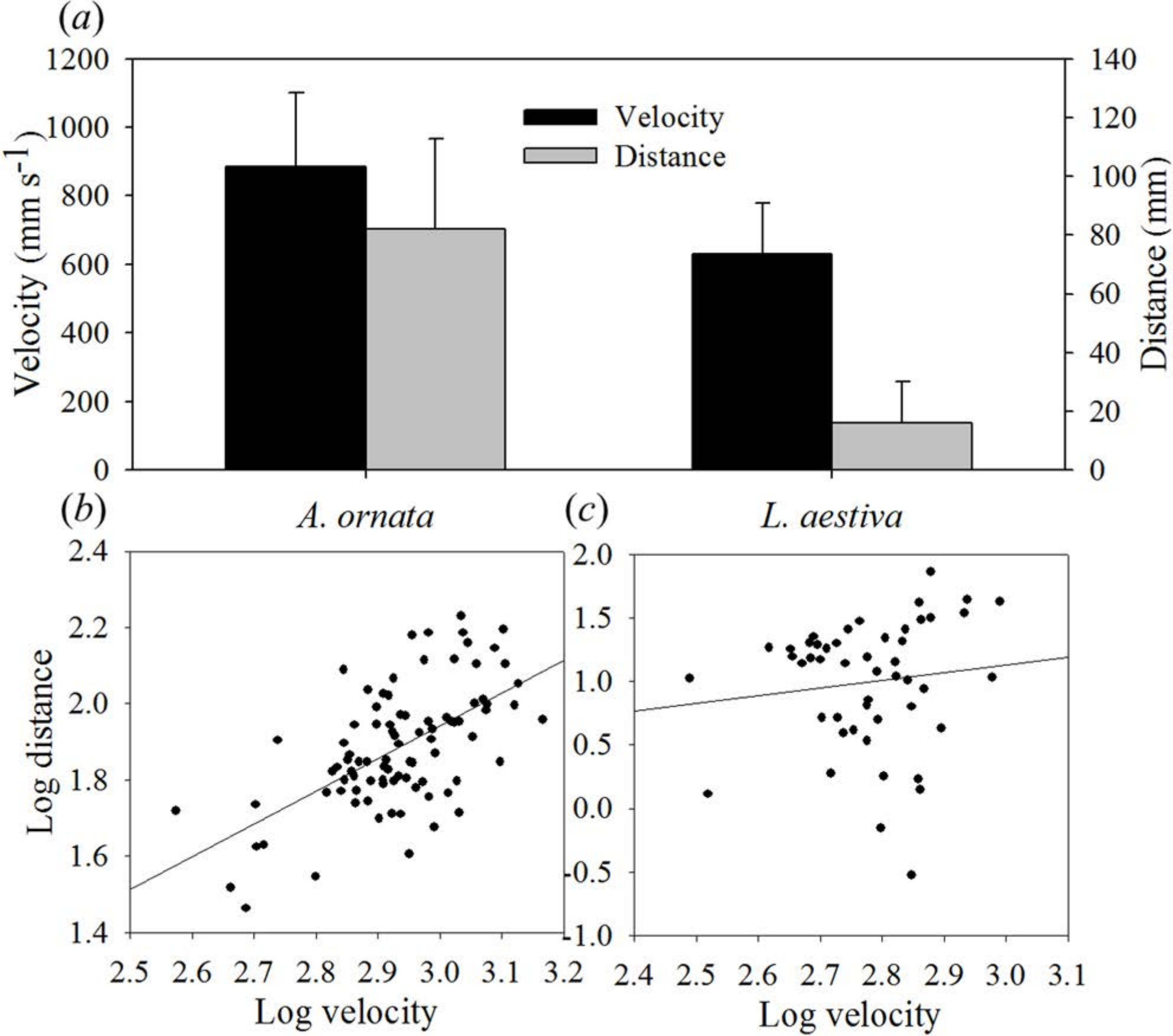
(a)
Velocity
Distance
Velocity (mm s-1)
Distance (mm)
1200
1000
800
600
400
200
0
140
120
100
80
60
40
20
0
(b)
A. ornata
(c)
L. aestiva
Log distance
Log velocity
Log velocity
2.4
2.2
2.0
1.8
1.6
1.4
2.5 2.6 2.7 2.8 2.9 3.0 3.1 3.2
2.0
1.5
1.0
0.5
0.0
-0.5
-1.0
2.4 2.5 2.6 2.7 2.8 2.9 3.0 3.1

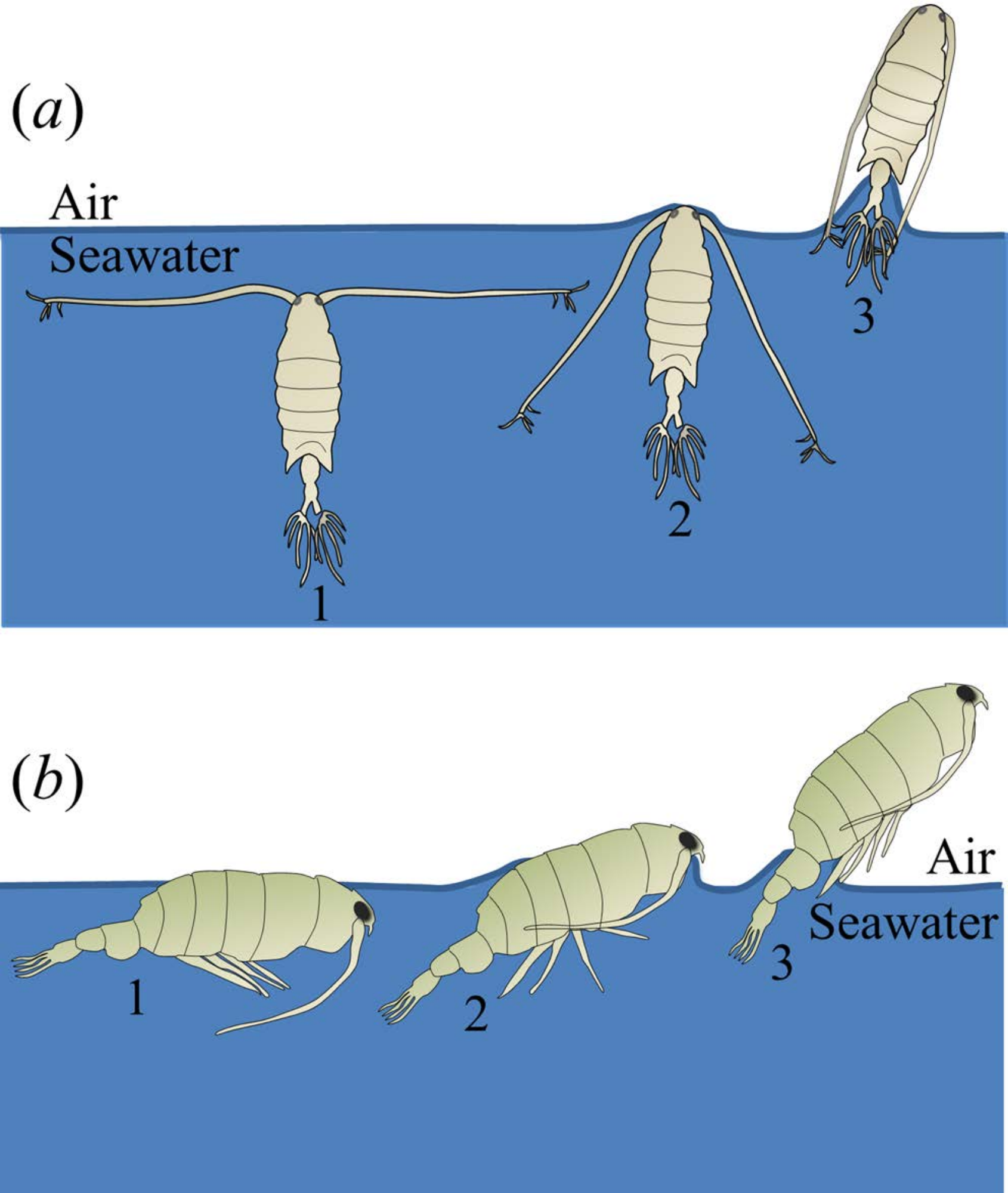
(a)
Air
Seawater
1
2
3
(b)
Air
Seawater
1
2
3

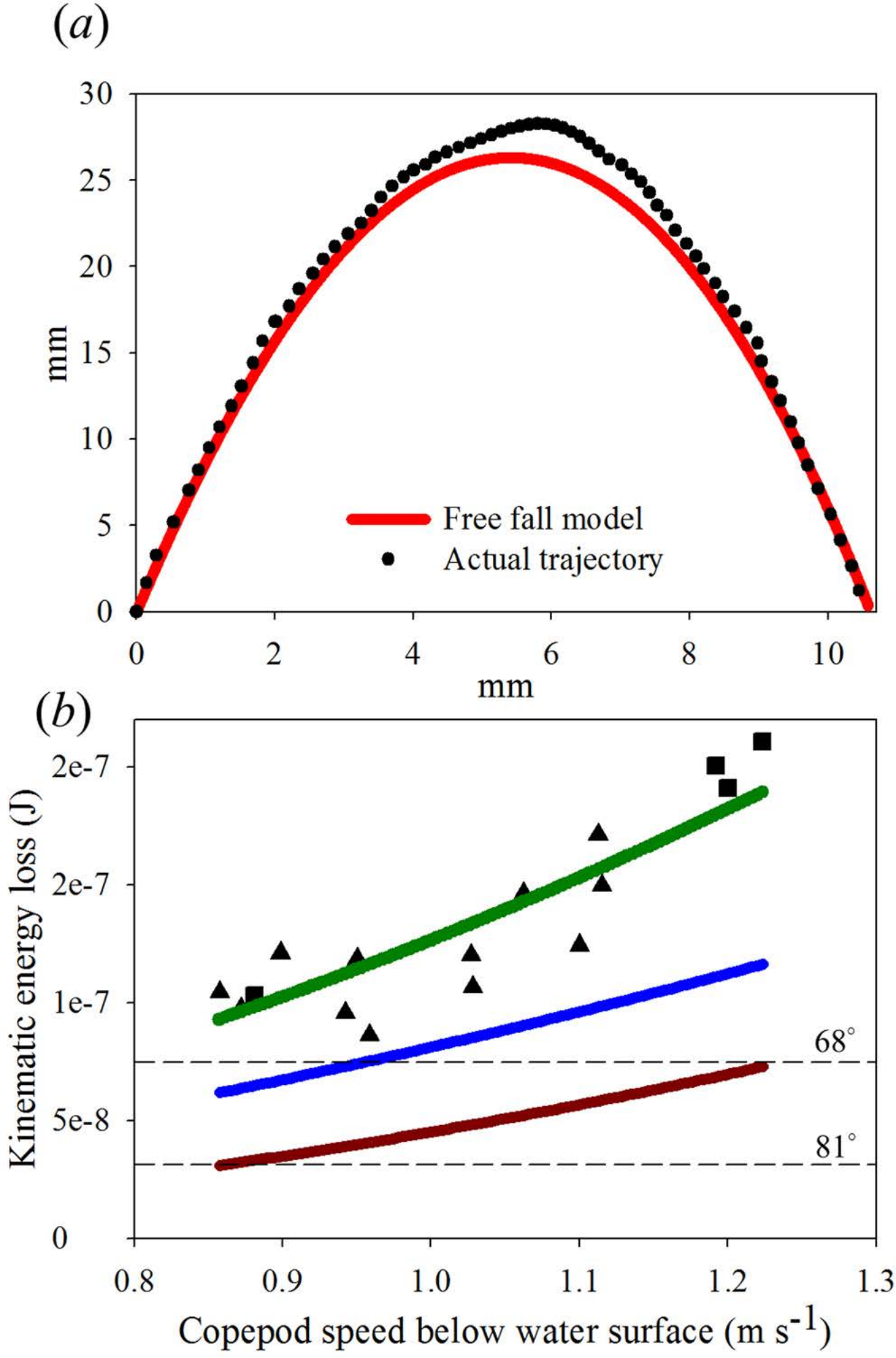
(a)
30
25
20
15
10
5
0
mm
Free fall model
Actual trajectory
0
2
4
6
8
10
mm
(b)
2e-7
2e-7
1e-7
5e-8
0
Kinematic energy loss (J)
68°
81°
0.8
0.9
1.0
1.1
1.2
1.3
Copepod speed below water surface (m s-1)